SENSING OF METEOROLOGICAL VARIABLES
BY LASER PROBE TECHNIQUES

SEMIANNUAL REPORT

NATIONAL AERONAUTICS AND SPACE ADMINISTRATION

Grant NGR-22-009-131

covering the period February 1 — July 31, 1967

August 30, 1967

N67-38030

(ACCESSION NUMBER)

(THRU)

(CODE)

(CATEGORY)

13

(PAGES)

CR#88972

(NASA CR OR TMX OR AD NUMBER)

FACILITY FORM 602

Submitted by: Giorgio Fiocco

Massachusetts Institute of Technology
Research Laboratory of Electronics
Cambridge, Massachusetts

SUMMARY OF RESEARCH

1. Experiments to Determine the Aerosol Content of Air from Spectral Analysis of Laser Echoes

Spectral analysis of the echoes obtained from atmospheric constituents in optical radar experiments yields information related to wind motion, temperature, and composition.

We have performed some preliminary laboratory experiments, in which the spectrum of the scattered radiation is analyzed in order to provide a measurement of the aerosol component.

The laser is a Spectra Physics Model 130 with a nominal output of 0.7 mW at 6328 Å, with a hemispherical resonator configuration producing a single transverse mode with several longitudinal modes separated approximately by 0.0067 Å (since the resonator length is 30 cm). Although we have evidence of thermal drift of these modes, we have assumed that, by integrating several scans and allowing each scan to be sufficiently slow, the laser spectral output could be considered to be independent of time.

The laser beam was passed through an aperture to limit the amount of fluorescence radiation emitted, and then passed through a synchronized attenuator the function of which will be described below. Light scattered in a volume approximately represented by a cylinder of 0.5-cm diameter and 15-cm length was observed with a receiving telescope located 3.6 m from the scattering volume at a scattering angle of 177.2°. The collected light was collimated and then passed through a pressure-scanned Fabry-Perot interferometer.

The Fabry-Perot interferometer has plates of 3.75-cm diameter and is flat to a nominal surface accuracy of $1/100\lambda$, coated with a broadband, dielectric coating of reflectivity 94% at 6328 Å, and separated by INVAR spacers of different thicknesses. In the particular experiments described below, the spacer thicknesses were 1 and 2 cm. The chamber was filled with N_2, and the pressure inside was controlled by passing N_2 through a

controlled leak and a flowmeter. The free spectral range of the interferometer with a 1-cm spacer is $0.20\,\overset{\circ}{A}$ at $6328\,\overset{\circ}{A}$, and the finesse achieved by passing light through a circular area ~2 cm in diameter was estimated to be approximately 20. The focal length of the fringe-forming lens was 17.2 cm, and the scanning aperture was a circular hole, 0.56 mm in diameter. The size of the scanning aperture was matched to the focused image of the scattering volume.

The photomultiplier was an EMI 9558A cooled with methanol previously refrigerated to dry ice temperature. The amplified photoelectron pulses in a 1-sec time interval were then counted with a TSI Model 385-R counter, and then printed.

To allow for the possibility that the laser spectrum or instrumental response might change during the course of the measurements, the following scheme was used to afford continual comparison of the radiated and scattered spectra. A rotating wheel with portions of the surface cut away was placed at the center of the scattering volume so that the telescope was presented at alternate count intervals with scattering from the medium, and scattering from the flat wheel surface. In order to present the detector with comparable signal levels, the synchronous attenuator mentioned above was used to attenuate the beam by several orders of magnitude with a neutral density filter whenever the wheel surface was in position. Admittedly, an instrument requiring such a device at the location of the scattering volume would not be very suitable for remote sensing. Its presence is not essential, however, and it is not a very difficult problem to provide an internal rather than an external reference.

The preliminary experiments carried out consisted of measuring the spectrum of light scattered from air in the laboratory containing natural aerosol particles, and air containing an artificially produced dense fog.

The laboratory air contains an unknown amount of aerosols, presumably small, since such air is kept circulating through air conditioning filters and the room has limited access and no windows on the outside. The artificially produced fog was obtained by blowing moist air through dry ice, and filled approximately the same scattering volume as was observed

2

in the case of ambient air. The cross section per unit volume of the fog is many times that of the air; hence, the spectrum of the fog should exhibit negligible broadening, because of the high concentration of aerosol particles and the response from the fog may be considered a measure of the instrumental response.

To a first approximation, the spectrum of the light scattered from the fog should be identical to the spectrum of the light scattered from the wheel surface. Since the scattering volume for the fog is extended in space, however, the instrumental response in the two cases is not quite identical. For one thing, the spatial distribution of illumination in the plane in which the fringes are formed is different and may produce a modulation of the output. For another, the finesse of the Fabry-Perot depends on the amount and portion of the etalon utilized, and this also differs in the two cases. Thus, although the spectrum of light scattered from the wheel is useful for comparative purposes, it should not be assumed to be identical to the instrumental response.

The data taken are shown in Figs. 1, 2, and 3. Figure 1 (curve a) represents an average of 3 scans obtained by using ambient air and the 2-cm spacer in the Fabry-Perot. Figure 2 (curve a) represents an average of 10 scans obtained by using ambient air and the 1-cm spacer in the Fabry-Perot. Figure 3 (curve a) represents a single scan obtained from the fog by using the 2-cm spacer. Curves b in Figs. 1, 2, and 3 represent the simultaneous spectral scans obtained from the wheel surface (target). The noisiness in such curves is due to the nonstationary character of the cross section of the aerosol particles, the thermal fluctuations of the laser spectrum, and shot noise introduced by the photodevice. The signal level was substantially higher in Fig. 3, and consequently the shot-noise fluctuations are greatly reduced. In spite of the noisiness of the data, the broadening effect is evident in Figs. 1 and 2. The increased resolution used in Fig. 1 makes the effect even more noticeable. An analysis of the curve indicates that the dust-to-air ratio $\Re$ was approximately one.

Experiments with improved resolution and the use of two laser

frequencies are in preparation. It is hoped that information on the aerosol size distribution may be obtained in this manner.
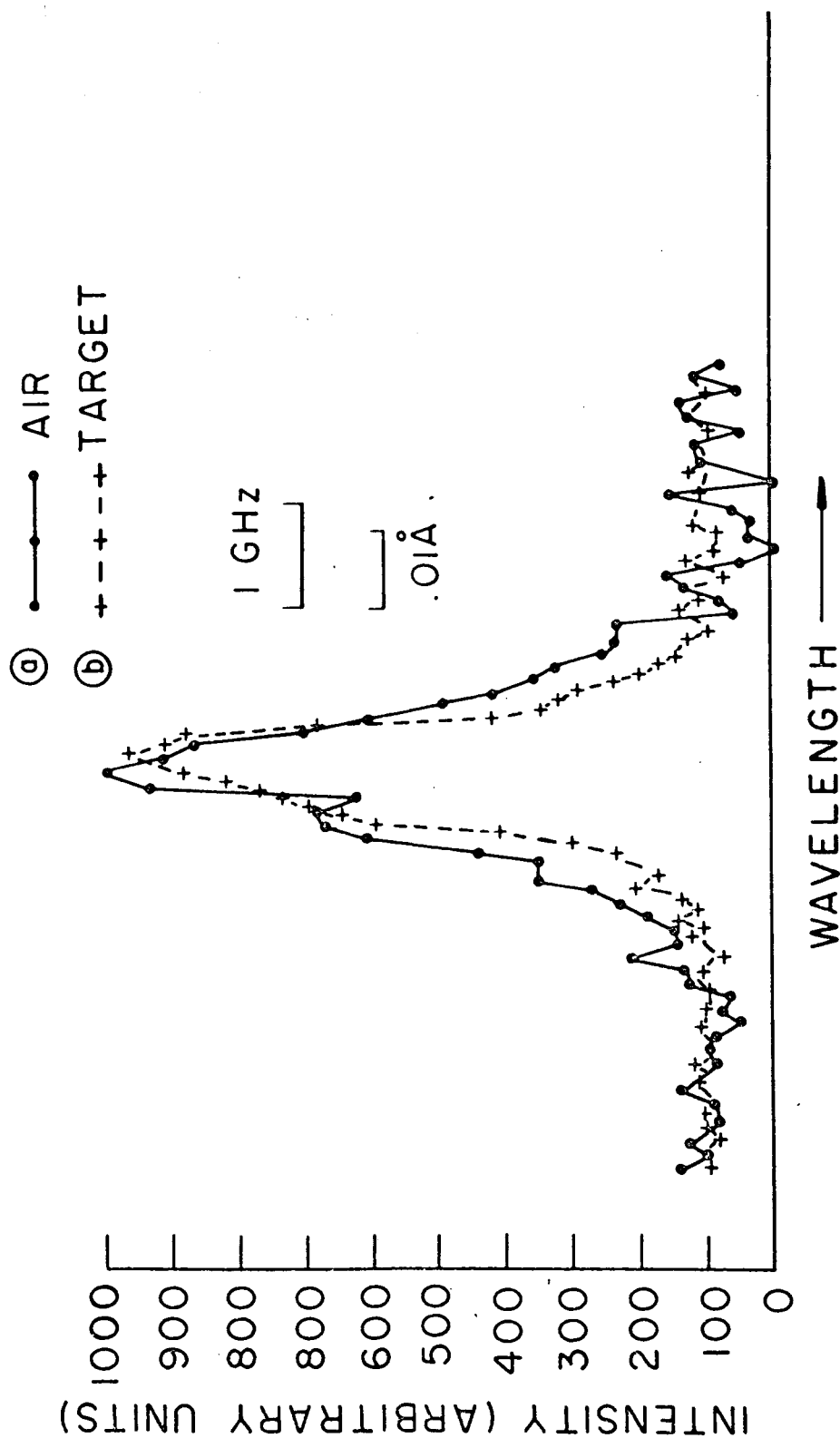
J. B. De Wolf, G. Fiocco

Fig. 1. Spectrum of light scattered from laboratory air and a reference target as observed with a Fabry-Perot interferometer having a 2-cm spacer. The ordinate distance is proportional to the photoelectron counts obtained in a 1-sec interval while scanning.
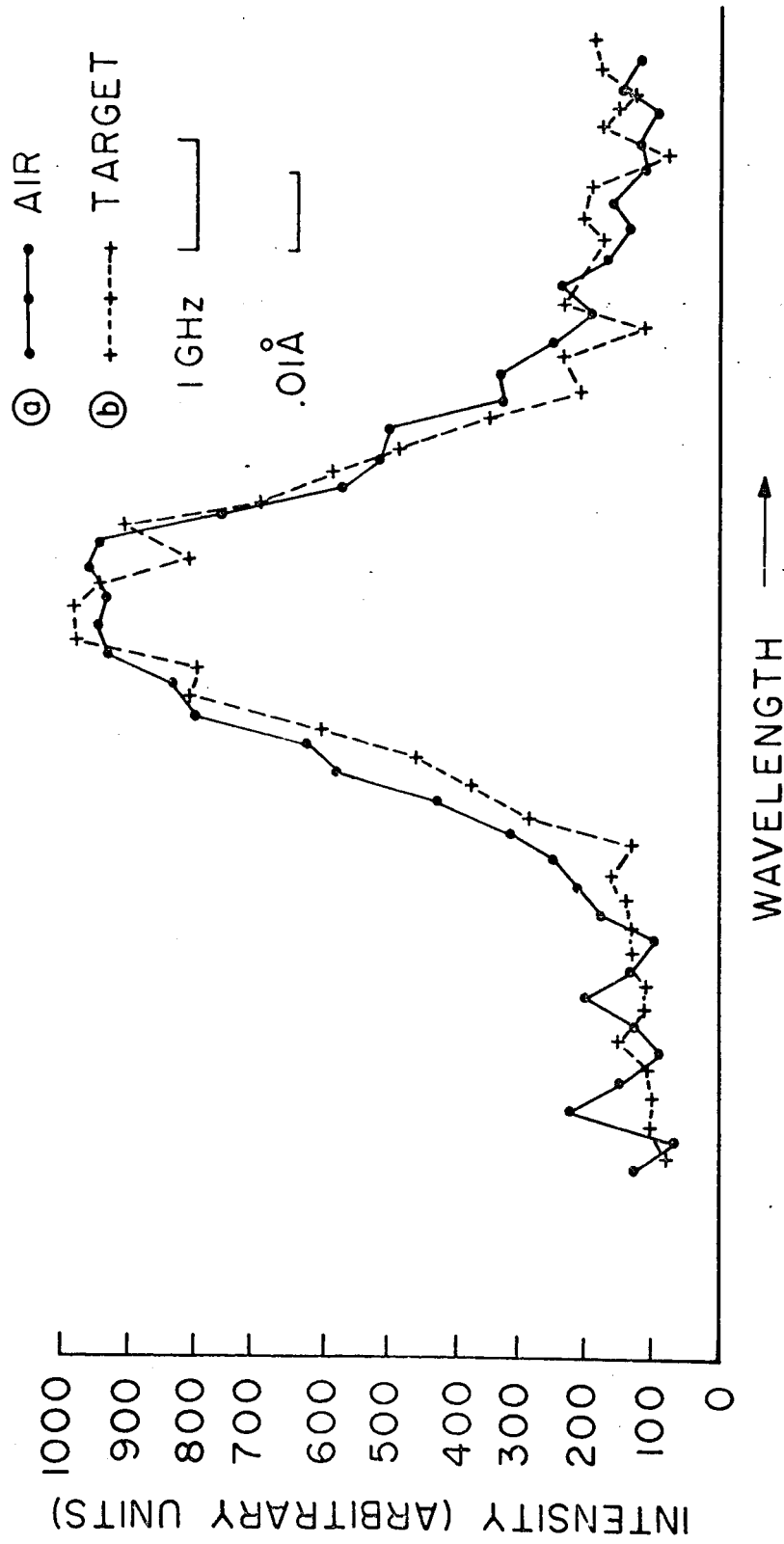
5

Fig. 2. Spectrum of light scattered from laboratory air and a reference target as observed with an FPI having a 1-cm spacer.
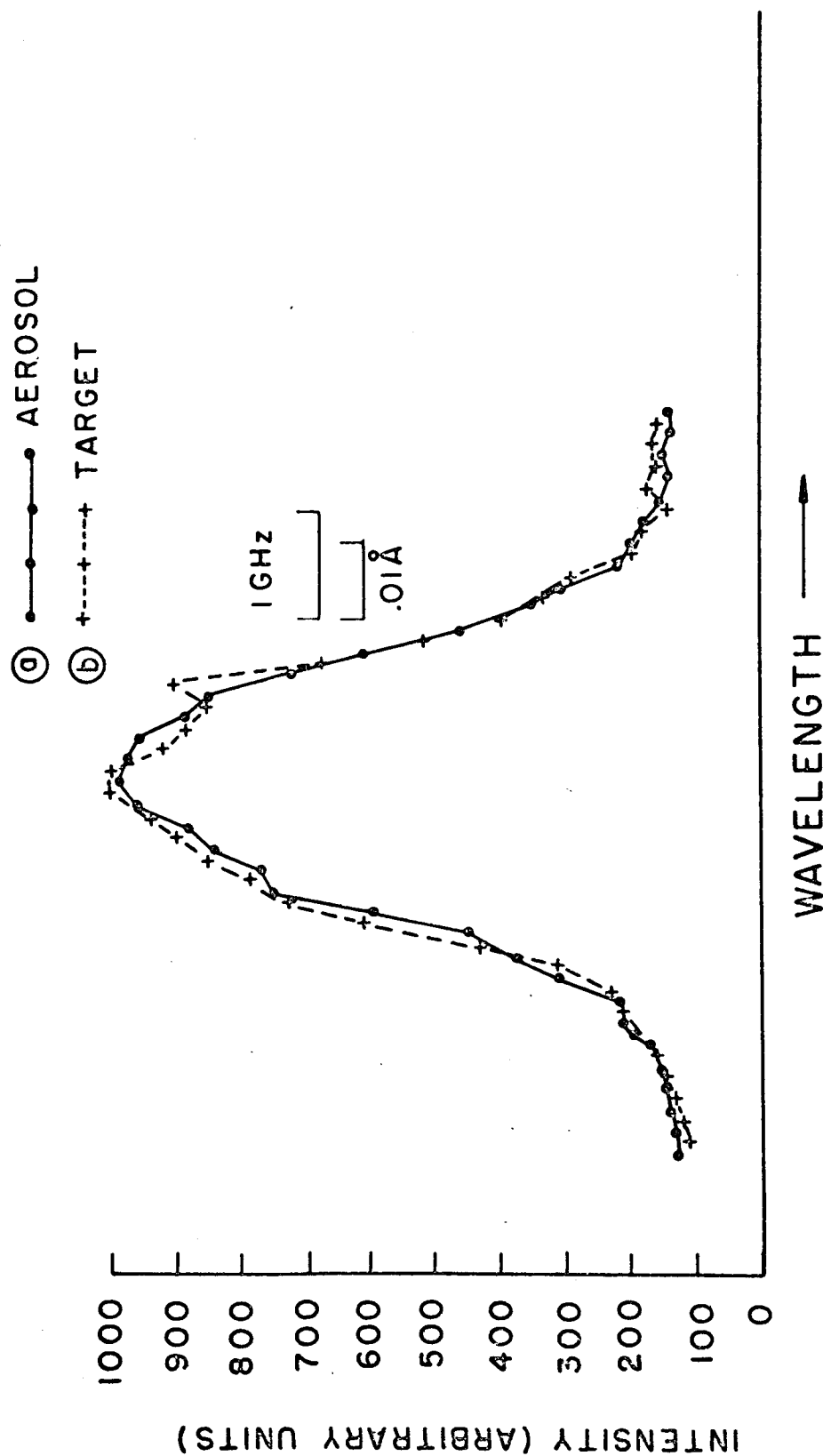
Fig. 3. Spectrum of light scattered from an artificially produced fog as observed with an FPI having a 1-cm spacer.

7

2. Measurement of the Density and Temperature of the Electrons in a Low-Density Reflex Discharge by Scattering of Continuous-Wave Ar$^+$ Laser Light.

An experiment to measure the electron temperature and density in a laboratory discharge by scattering of continuous-wave Ar$^+$ laser radiation at 4880 Å has been successfully carried out by Harry C. Koons and Giorgio Fiocco.

The power now available from cw lasers operating in the visible region of the spectrum is several orders of magnitude lower than the pulsed output made possible by the ruby laser. Thus, in plasma scattering experiments the level of the scattered laser radiation will be small compared with the level of the background plasma radiation; thus in general, long integration times are required before statistical evidence of detection can be achieved. At the present stage of development, however, stable, continuous-wave lasers may, in some cases, offer advantages over the pulsed high-power ruby laser.

In fact, the characteristics of the discharge under consideration may prevent the use of high radiation levels. Changes in the relative population of excited states, or an increase in ionization may be effected by high-intensity radiation. Some evidence for these effects was found in previous experiments by Thompson and Fiocco with a hollow cathode discharge. Such effects would be most likely to occur in under-dense plasmas. Significantly, much of the work by other investigators has been directed toward the investigation of highly ionized, hot plasmas.

In some experiments, a continuous-wave laser source may have several advantages over pulsed lasers. They allow the use of counting or synchronous detector systems; the output power is, at present, considerably more stable than the power per pulse in a ruby laser; the available wavelength stability and high degree of coherence offer considerable advantages for the narrow-band spectral analysis that is necessary for measuring ion temperatures and collective effects; they are also free of thermal drifts which simplifies electron density and temperature measurements.

8

A schematic diagram of the experiment is shown in Fig. 4. The light from an Ar^+ laser was focused into the plasma, and the scattered radiation was observed at a scattering angle of approximately 8°. Both plasma current and laser light were modulated in order to permit synchronous detection of the scattered radiation and rejection of the background. The spectrum of the scattered light was obtained by rotating a narrow-band interference filter.

The plasma was formed by a reflex discharge in helium, at a pressure of 2.5×10^{-3} Torr. The value of DC current through the discharge was $I = 1.8$ amps, with an axial magnetic field of $B = 0.1$ Wb/m^2. The gas was then approximately 10% ionized at the center of the discharge. The ion density at the center obtained from Langmuir probe curves was approximately 10^{19} m^{-3}. The electron temperature was also measured by a probe. The value obtained by averaging four probe determinations was 1.30 ± 0.37 eV.

The Ar^+ laser, built by Space Rays, Inc. has a total power output at several wavelengths of approximately 2 watts. The output power available at 4880 Å was approximately 0.5 watt.

For the particular values of the various parameters at which the experiment was carried out, the scattered spectrum has a Gaussian shape centered about the wavelength of the incident radiation with a width determined by the electron temperature. The output of the lock-in amplifier as a function of the angle of the rotation filter is shown in Fig. 5. By using the value for the width obtained from the scattering measurements, the electron temperature obtained is 1.1 eV. This is in good agreement with the temperature determined by the probe data.

The electron density may be determined from the total number of photons scattered into the solid angle of the detector if the efficiency of the optical detection system and electronics is known. Using values for all parameters which were either measured in our laboratory or provided as calibrations by the manufacturers, we obtained 9.1×10^{18} m^{-3} as the value for electron density from the scattering data, which is also in good agreement with the probe measurements.

We plan to add a Fabry-Perot interferometer to the detector system at a smaller scattering angle. This will allow narrow-band spectral measurements to be made from which we might be able to determine the ion density and observe collective effects in the plasma.

The experimental arrangement will also be used to measure scattering cross sections of air for a better understanding of Brillouin scattering effects and of the role of aerosols in atmospheric scattering experiments.
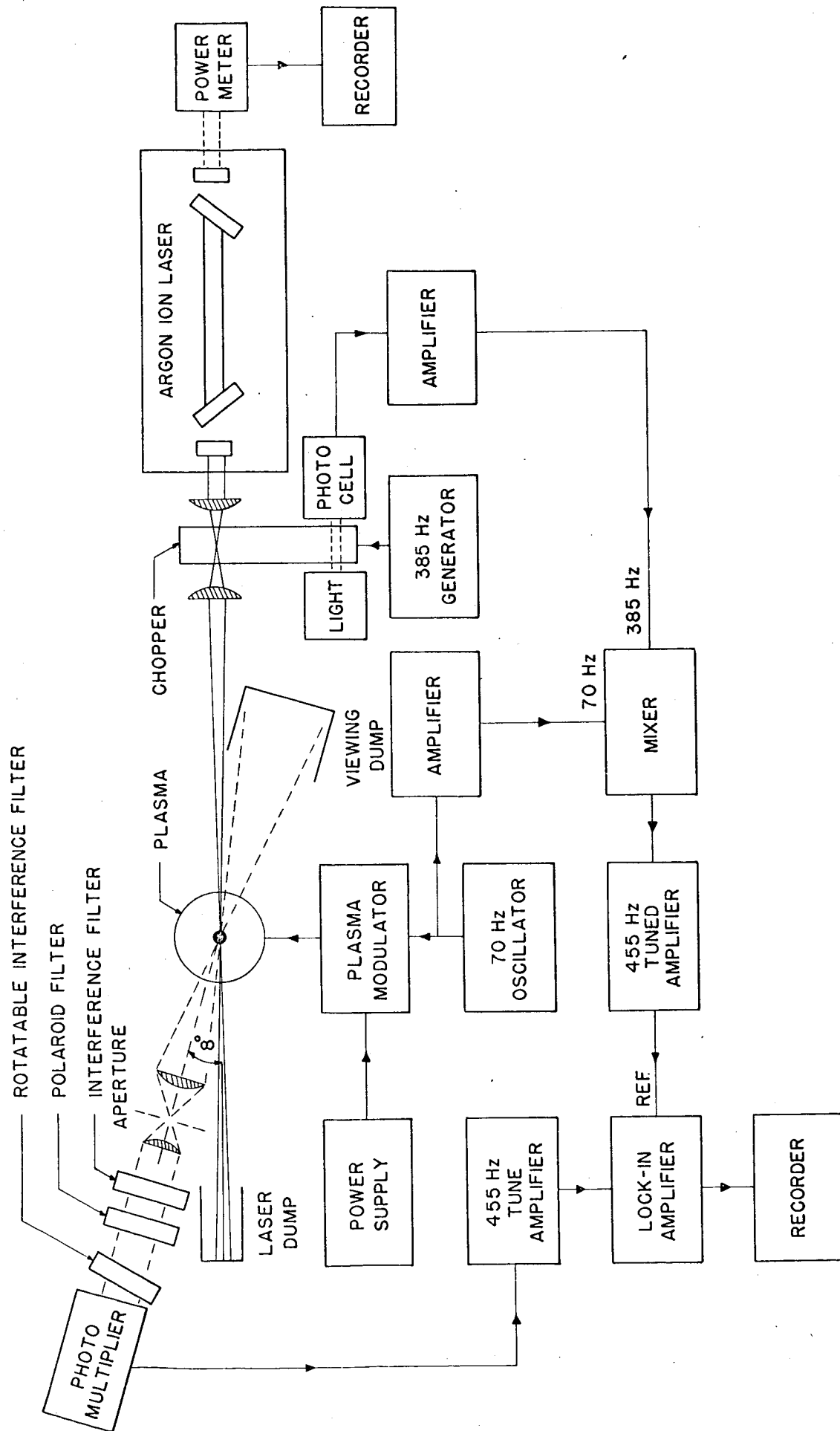
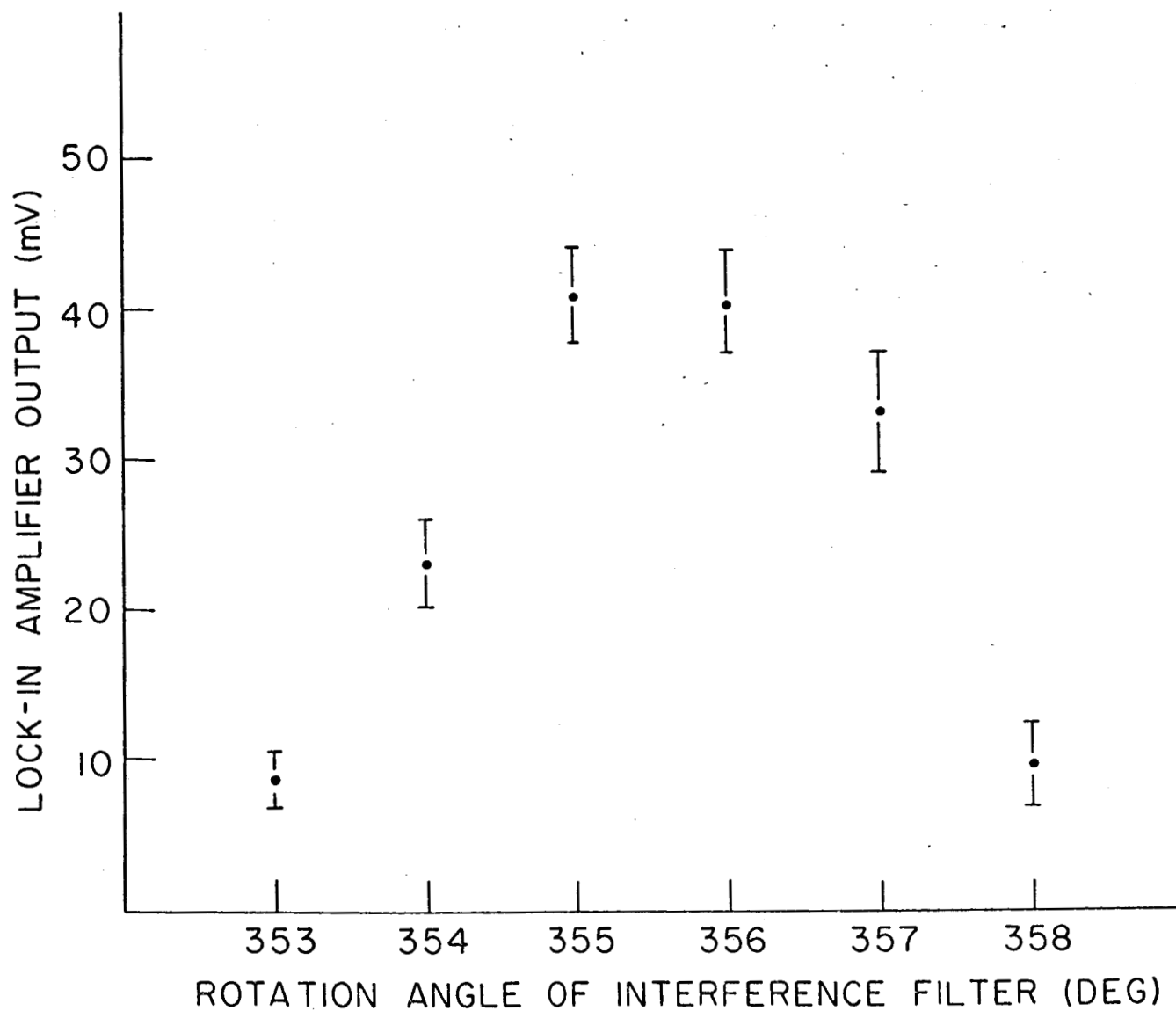Fig. 4　Schematic diagram of the experimental apparatus

11

Fig. 5 Scattering intensity vs. the rotation angle of the interference filter.
The angle indicated in the figure is taken with respect to an arbitrary zero.